Chinese Chemical Letters 32 (2021) 2390–2394

Contents lists available at ScienceDirect

Chinese Chemical Letters

journal homepage: www.elsevier.com/locate/cclet

Communication

The density of surface ligands regulates the luminescence of thiolated gold nanoclusters and their metal ion response

Jie Xu[a], Juanmin Li[a], Wencheng Zhong[a], Mengyao Wen[a], Gleb Sukhorukov[b,c], Li Shang[a,b,*]

[a] State Key Laboratory of Solidification Processing, School of Materials Science and Engineering, Northwestern Polytechnical University and Shaanxi Joint Laboratory of Graphene (NPU), Xi'an 710072, China
[b] NPU-QMUL Joint Research Institute of Advanced Materials and Structures (JRI-AMAS), Northwestern Polytechnical University, Xi'an 710072, China
[c] Materials Research Institute, School of Engineering and Materials Science, Queen Mary University of London, London E1 4NS, United Kingdom

ARTICLE INFO

Article history:
Received 25 December 2020
Received in revised form 18 February 2021
Accepted 19 February 2021
Available online 22 February 2021

Keywords:
Gold nanoclusters
Luminescence enhancement
Ligand density
Thermal treatment
Metal ion

ABSTRACT

The fascinating luminescence properties of gold nanoclusters (AuNCs) have drawn considerable research interests, and been widely harnessed for a wide range of applications. However, a fundamental understanding towards ligand density's role in the luminescence properties of these ultrasmall AuNCs remains unclear yet. In this communication, through systematic investigation of surface chemistries of glutathione-protected AuNCs (GSH-AuNCs) with different density of GSH as well as other thiolates, it is discovered that the density of surface ligands can significantly regulate the luminescence properties of AuNCs. Fluorescence lifetime spectroscopy and X-ray photoelectron spectroscopy showed that AuNCs with a higher density of electron-rich ligands facilitate their luminescence generation. Moreover, differences in the surface coverage of AuNCs can also affect their interactions with foreign species, as illustrated by significantly different fluorescence quenching capability of GSH-AuNCs with different ligand density towards Hg^{2+}. This study provides new insight into the intriguing luminescence properties of metal NCs, which is hoped to stimulate further research on the design of metal NCs with strong luminescence and sensitive/specific responses for promising optoelectronic, sensing and imaging applications.

Metal nanoclusters (NCs) as a novel type of luminescent nanomaterials have attracted extensive attention because of their unique properties such as ultrasmall size, low toxicity, excellent biocompatibility and good photostability [1–3]. Until now, luminescent metal NCs have been widely used in the fields of optical sensing [4–7], bioimaging [8,9], light energy conversion [10], light-emitting devices (LED) [11,12] and biomedical research [13–15]. Nevertheless, the luminescence quantum yield (QY) of the most currently reported metal NCs (usually < 10%) is relatively lower than many other fluorophores such as organic dyes and quantum dots. Therefore, a great deal of efforts have been devoted in recent years to improve their luminescence QY *via* different strategies, and more importantly to understand the origin and underlying luminescence mechanism.

Among the various types of metal NCs, gold nanoclusters (AuNCs) stabilized with thiolate ligands, have been a topic of intense research [16–18]. These thiolated AuNCs typically exhibit excellent stability owing to strong gold-sulfur bonds, tunable emission wavelength and easy purification after the synthesis, making them promising for many biological applications. These thiolate ligands not only provide a good protection for stabilizing AuNCs, but also regulate their physicochemical properties and subsequent utilization. In particular, recent studies revealed that the luminescence of thiolated AuNCs is strongly influenced by their surface ligands [19–21]. For example, Jin *et al.* [22] reported that the surface ligands can influence the luminescence of AuNCs in two different ways: (i) charge transfer from the ligands to the metallic core (*i.e.*, ligand-to-metal charge transfer, LMCT) through Au-S bonds, and (ii) direct donation of delocalized electrons from electron-rich atoms/groups of the ligands to the metal core.

Indeed, both experimental and theoretical studies indicate that highly luminescent AuNCs can be obtained by reasonably engineering ligand-Au core interactions [23,24]. One commonly adopted approach is the design of optimal ligands that can

* Corresponding author at: State Key Laboratory of Solidification Processing, School of Materials Science and Engineering, Northwestern Polytechnical University and Shaanxi Joint Laboratory of Graphene (NPU), Xi'an 710072, China.
E-mail address: li.shang@nwpu.edu.cn (L. Shang).

https://doi.org/10.1016/j.cclet.2021.02.037

promote the luminescence generation process. In contrast, recent studies underlined the potential role of ligand coverage on the luminescence properties of thiolated AuNCs [25]. For example, Liu *et al.* [26] reported that different coverage of ligands on gold nanoparticles (AuNPs) can exhibit different emission colors independent of core sizes. Moreover, researchers found that the coverage density of surface ligands significantly influences the biological activity [27] and stimuli-responsive performances of AuNPs [28]. Despite considerable efforts in these previous studies, fundamental understanding towards the role of surface ligands' density on the optical properties of AuNCs remains mystery yet, but of immense importance [29,30]. Herein, with glutathione-protected AuNCs (GSH-AuNCs) as the example, we systematically exploited the role of ligand density on the optical properties of AuNCs with a library of different thiolate ligands. Moreover, we investigated the effect of ligand density on the optical response behaviors of GSH-AuNCs towards metal ions (*i.e.*, Hg^{2+}).

GSH-AuNCs with different ligand densities were first synthesized based on well-established strategies. GSH-AuNCs with a relatively lower density (denoted as *l*-GSH-AuNCs, Fig. 1a) were directly prepared through the reduction of $HAuCl_4$ in the presence of GSH. Further thermal treatment of *l*-GSH-AuNCs with excess amount of GSH at 50 °C for 6 h yields AuNCs with a higher ligand density (denoted as *h*-GSH-AuNCs, Fig. S1 in Supporting information). X-ray photoelectron spectroscopy (XPS) was first employed to semi-quantitatively estimate the relative density of GSH on the surface of AuNCs (Fig. 1b). The relative ligand density of *l*-GSH-AuNCs, calculated based on the ratio of the integrated peak areas of Au and S in XPS spectra (n_S/n_{Au}), was 0.89, which is lower than that of *h*-GSH-AuNCs (0.96). Further characterization with ICP-OES also revealed a higher density of GSH on the surface of *h*-GSH-AuNCs than that of *l*-GSH-AuNCs. Meanwhile, TEM images showed the core size of *l*-GSH-AuNCs and *h*-GSH-AuNCs is 1.7 ± 0.2 nm and 1.6 ± 0.2 nm, respectively (Figs. 1c and d). This result suggests that the size of GSH-AuNCs remain essentially unchanged upon thermal treatment. Together, the above characterization confirmed successful synthesis of two GSH-AuNCs with different ligand density as expected.

We next investigated the effect of the ligand density on the optical properties of these GSH-AuNCs. As shown in Fig. S2 (Supporting information), the absorption spectra of *l*-GSH-AuNCs and *h*-GSH-AuNCs both display a featureless decay in the UV–vis region. Compared with the absorption spectra of *l*-GSH-AuNCs, there is only a slight decrease in the region below 500 nm for *h*-GSH-AuNCs, which is likely due to the difference in the electronic interactions between the surface ligand and the kernel. In stark contrast, the fluorescence properties of both GSH-AuNCs are significantly different. As seen in Fig. 2a, the fluorescence intensity of *h*-GSH-AuNCs is about 2.2 fold stronger than that of *l*-GSH-AuNCs. Note that the fluorescence intensity has been normalized by the absorbance value at the excitation wavelength, thus this increase reflects the QY enhancement directly. Meanwhile, the maximum excitation and emission wavelength remain almost unchanged independent of their surface ligand density, which is in good agreement with previous studies on the luminescence mechanism of AuNCs. Particularly, Xie *et al.* [31] revealed that the kernel structure of AuNCs is the primary factor to determine the energy of the luminescence, while the surface Au-ligand interactions are the key to determine the QY of AuNCs.

Fluorescence lifetime was further measured to understand the underlying reason contributing to their different fluorescence intensity. As seen in Fig. 2b, concomitant with the intensity increase, the fluorescence decay of *h*-GSH-AuNCs is longer than that of *l*-GSH-AuNCs. Further fitting the decay with a biexponential decay function yields two lifetime components. Compared with that of *l*-GSH-AuNCs, the fraction of the long lifetime component (τ_2) for *h*-GSH-AuNCs is significantly increased from 54.75% to 71.69%, together with a decrease in the short lifetime component (τ_1) from 45.25%–28.31% (Fig. 2c). The microsecond radiative lifetimes of these AuNCs suggested that their emission could be attributed to a LMCT [S→Au(I)] effect from the sulfur atom in the thiolate ligands to the Au center [32]. Such a LMCT process is believed to affect the excited state radiative relaxation dynamics [33]. Because of more GSH ligands on the surface of *h*-GSH-AuNCs, they possess a stronger LMCT effect than that of *l*-GSH-AuNCs, thus the electron radiative relaxation dynamics of *h*-GSH-AuNCs are slower. Meanwhile, the existence of more surface ligands can provide a better passivation of the surface defects, which will also likely enhance the luminescence of AuNCs *via* diminishing non-radiative processes.

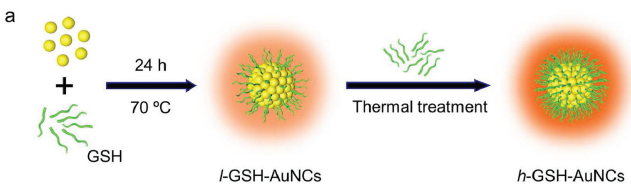

b

	l-GSH-AuNCs	*h*-GSH-AuNCs	*h*-GSH / *l*-GSH (%)
XPS (n_S / n_{Au})	0.89 ± 0.03	0.96 ± 0.06	107.87
ICP (c_S / c_{Au})	0.84 ± 0.02	0.88 ± 0.04	104.76

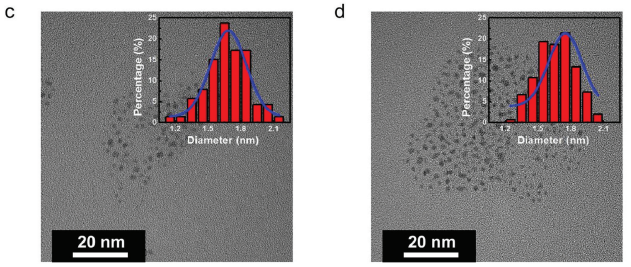

Fig. 1. (a) Schematic illustration of the synthesis of GSH-AuNCs with different ligand densities. (b) Characterization of the relative ligand density of GSH-AuNCs by XPS and ICP-OES. (c, d) are representative HR-TEM images of *l*-GSH-AuNCs and *h*-GSH-AuNCs, respectively. Insets in the upper right are size histograms based on TEM images.

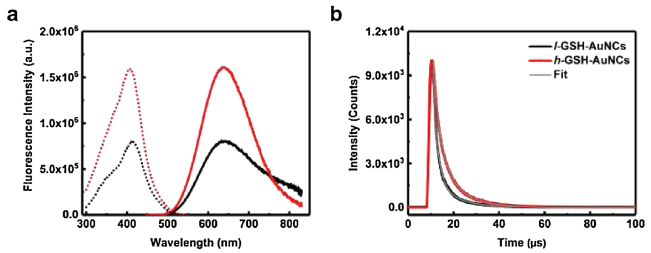

c

Sample	τ_1 (μs)	α_1 (%)	τ_2 (μs)	α_2 (%)	τ_{av} (μs)
l-GSH-AuNCs	2.00 ± 0.03	45.25 ± 0.54	9.04 ± 0.07	54.75 ± 0.54	7.95 ± 0.05
h-GSH-AuNCs	2.74 ± 0.01	28.31 ± 0.48	9.22 ± 0.01	71.69 ± 0.48	8.54 ± 0.02

Fig. 2. (a) Fluorescence excitation (dotted line) and emission (solid line) spectra of the *l*-GSH-AuNCs (black line) and *h*-GSH-AuNCs (red line) in aqueous solution. (b) Photoluminescence decay profiles of *l*-GSH-AuNCs (black line) and *h*-GSH-AuNCs (red line) in aqueous solution, and the corresponding fitted curves by biexponential decay functions. (c) Summary of lifetimes of both GSH-AuNCs (λ_{em} = 638 nm and λ_{ex} = 412 nm).

In order to evaluate the possible effect of ligand density on the chemical structure of AuNCs, XPS spectra of both GSH-AuNCs were measured (Fig. S3 in Supporting information). The binding energy (BE) of Au $4f_{7/2}$ and Au $4f_{5/2}$ for *l*-GSH-AuNCs falls in 84.5 eV and 88.2 eV, respectively, which is characteristic of AuNCs with the coexistence of Au(0) and Au(I) in the clusters [34,35]. The BE of Au 4f for *h*-GSH-AuNCs remains almost unchanged, suggesting a negligible influence of ligand density on the valence states of Au. Moreover, a similar behavior was observed for the S 2p spectra of GSH-AuNCs, where the BE of the doublet peak attributing to S $2p_{3/2}$ and S $2p_{1/2}$ at 162.6 eV and 164.1 eV remain unchanged for both AuNCs (Fig. S3b in Supporting information). However, we note that the relative percentage of oxidized sulfur, locating at 168.2 eV, in *h*-GSH-AuNCs (22%) is higher than that of *l*-GSH-AuNCs (18%), indicating the presence of more oxidized sulfur species in AuNCs with a higher ligand density. This is reminiscent of recent finding by Wang *et al.* that oxidation of lipoic acid-protected AuNCs upon dialysis treatment led to an enhanced luminescence [36], which is in good agreement with our present result. The underlying reason is believed to be similar as the introduction of a positive charge at ligand terminal groups [22,37]. The presence of more oxidized sulfur species (*i.e.*, SO_x) will increase the oxidation-induced polarization at the core-ligand interfaces.

The above results clearly demonstrated the important role of ligand density in defining the optical properties of AuNCs, and those with higher surface coverage exhibit enhanced luminescence. Our next question is whether the chemical structure of introduced foreign ligands on the cluster surfaces will influence the properties of final AuNCs. To clarify this question, we replaced GSH with other three custom-designed tripeptides: Lys-Cys-Gly (KCG), Glu-Cys-Lys (ECK) and Glu-Ala-Gly (EAG), during the thermal treatment of *l*-GSH-AuNCs (Fig. 3a). Since both KCG and ECK possess cysteine residues, thermal treatment of *l*-GSH-AuNCs in the presence of 10-fold excess amount of KCG and ECK will also result in AuNCs with higher ligand density. Indeed, as seen in Fig. 3b and Fig. S4 (Supporting information), fluorescence intensity of AuNCs was increased with the emission maximum unchanged for KCG and ECK, which is similar as that of *h*-GSH-AuNCs. In contrary, almost no change in the fluorescence of GSH-AuNCs was observed in the case of EAG. The main difference in the structure of EAG compared with GSH is the absence of the thiol group, suggesting the important role of cysteine in ensuring effective binding to gold surfaces. The difference in the fluorescence enhancement effect among GSH, KCG and ECK is apparently related to their chemical structures. Interestingly, we found that the fluorescence intensity of final AuNCs upon thermal treatment of these three tripeptides is parallel with their capability of donating electrons to the metal core *via* the Au-S bond (*i.e.*, charge transfer capability of the ligand) [22]. Ligand containing more electron-rich atoms (*e.g.*, N) or groups (*e.g.*, NH_2) has strong electron donating capability, and is more capable of pushing electron density to the sulfur atom (*i.e.*, $S^{\delta-}$) and hence affects the Au core through the Au-S bond, resulting in stronger fluorescence enhancement. Herein, compared with GSH, KCG replaces one of its electrophilic carboxylic acid with a primary amine group, thus leading to stronger fluorescence enhancement. While for ECK, despite containing one more amine group than that of GSH, it possesses relatively high steric hindrance of amine groups and produces relatively weak influence on the emission of AuNCs [28]. As a result, the fluorescence enhancement effect of ECK on *l*-GSH-AuNCs is less than that of GSH. In accordance with this mechanism, we found that thermal treatment of *l*-GSH-AuNCs with short-chain thiolates such as L-penicillamine (LPA), L-cysteine (L-Cys), mercaptosuccinic acid (MSA) and tiopronin (Tio) lead to a significantly decreased fluorescence (Fig. 3c and Fig. S5 in Supporting information). Note that these small thiolates possess less electron-rich groups than that of tripeptides like GSH. Thus possible ligand exchange of original GSH on the cluster surfaces with these small thiolates during the thermal treatment will cause fluorescence quenching.

Owing to their distinct fluorescence property and good biocompatibility, metal NCs have been widely exploited for various sensing applications [38,39]. In most sensing applications, the recognition of analytes greatly relies on their direct interactions with the surface of metal NCs. Thus, for AuNCs with different density of surface ligands, their recognition behavior towards foreign species is expected to be different. To testify whether this is

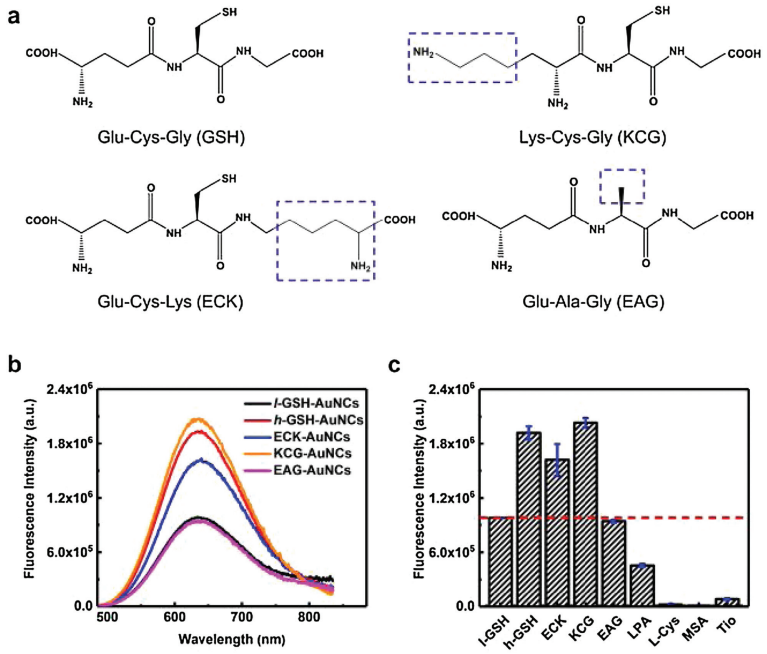

Fig. 3. (a) Chemical structures of GSH and other three GSH analogues. The main difference in the structure of these three analogues from GSH is labeled with dotted blue square. (b) Fluorescence emission spectra of *l*-GSH-AuNCs in aqueous solution before and after thermal treatment with 10× excess free tripeptides, taken with excitation at 412 nm. (c) The corresponding fluorescence intensity of GSH-AuNCs before and after thermal treatment with different thiolate ligands.

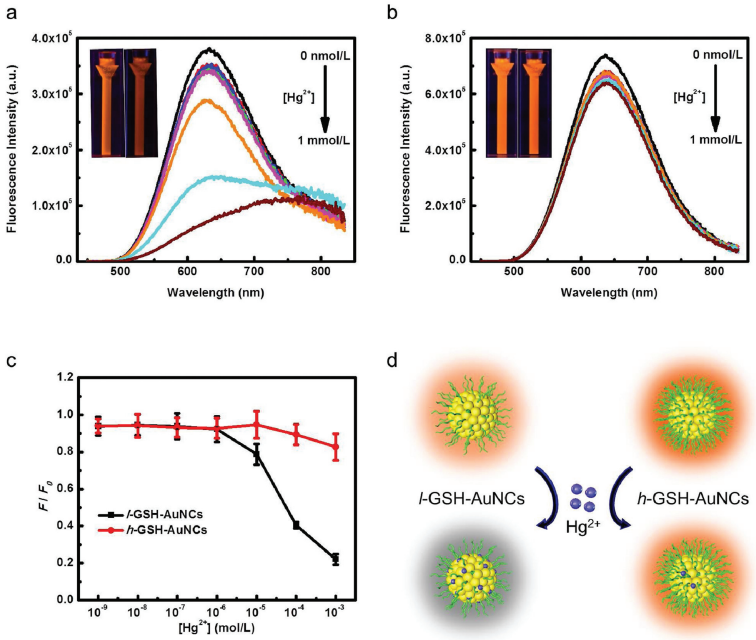

Fig. 4. Changes in fluorescence emission spectra of the as-prepared *l*-GSH-AuNCs (a) and *h*-GSH-AuNCs (b) with the addition of increasing concentrations of Hg^{2+} (from 0 nmol/L to 1 mmol/L), the inset displays the photos of GSH-AuNCs solution under 365 nm UV lamp irradiation in the absence (left) and presence (right) of 1 mmol/L Hg^{2+}. (c) Changes in F/F_0 value of *l*-GSH-AuNCs (black) and *h*-GSH-AuNCs (red) with the [Hg^{2+}], where F_0 and F are the fluorescence intensities of AuNCs at 638 nm in the absence and presence of Hg^{2+}, respectively. (d) Schematic illustration of the distinct fluorescence response of *l*-GSH-AuNCs and *h*-GSH-AuNCs towards Hg^{2+}.

the truth, we investigated the fluorescence response of both *l*-GSH-AuNCs and *h*-GSH-AuNCs towards one of the most commonly studied metal ions, Hg^{2+}. Previously, AuNCs protected by different ligands such as BSA [40], GSH [41] and lipoid acid [42] have been found to possess highly sensitive fluorescence response towards Hg^{2+}. According to these reports, Hg^{2+} can significantly quench the fluorescence of AuNCs *via* the high-affinity d^{10}-d^{10} metallophilic interaction between Au^{+} on the cluster surface and Hg^{2+} [40]. Indeed, as shown in Fig. 4a, the fluorescence intensity of *l*-GSH-AuNCs significantly decreased with the addition of Hg^{2+}. In the presence of 1 mmol/L Hg^{2+}, the fluorescence intensity decreased by over 80%, which can be clearly visualized upon illuminating the solution by UV light. However, when adding the same amount of Hg^{2+} into the aqueous solution of *h*-GSH-AuNCs that possess a higher ligand density, the phenomena is significantly different. As seen in Fig. 4b, the fluorescence intensity of *h*-GSH-AuNCs exhibit only slight decrease upon the addition of Hg^{2+}. Actually, in the presence of 1 mmol/L Hg^{2+}, the fluorescence intensity of *h*-GSH-AuNCs decreased by *ca.* 20%, which is much less than that of *l*-GSH-AuNCs (Fig. 4c). Apparently, the surface coverage of GSH-AuNCs has a strong influence on their interactions with Hg^{2+}. For those AuNCs with a high ligand density, contact of foreign species with the surfaces will be more difficult owing to steric hindrance effect. As a result, their binding affinity to these foreign species such as Hg^{2+} will be much weaker (Fig. 4d). We note that Hg^{2+} may also interact with the surface ligands directly and result in fluorescence quenching, but its effect is negilible compared with the strong metallophilic interactions. Our results suggest the possibility of engineering the surface responsive properties of metal NCs by controlling their surface chemistry, *i.e.*, ligand density. Particularly, when developing metal NC-based sensors, one can enhance the sensitivity by reasonably shrinking the surface ligands' density as long as sufficient stability can be ensured. Furthermore, the density of surface ligands is also expected to alter the formation of protein corona on the surfaces of these AuNCs, which will further affect their subsequent biological fates.

In summary, we showed that the ligand density on the surface of thiolated AuNCs plays an important role in defining their luminescence properties and their response towards foreign metal ions. AuNCs with a higher density of electron-rich ligands such as GSH and those GSH analogues facilitate their luminescence generation. However, the presence of other small thiolates with weak electron-donating capabilities will quench the luminescence of AuNCs, underlying the essential role of the chemical structure of ligands besides their density. Meanwhile, differences in the surface coverage of these ultrasmall AuNCs will affect their further interactions with foreign species such as Hg^{2+} ions. These findings not only advance our understanding about the structure-property relationship of these emerging luminescent metal NCs, but also provide important new avenues for designing robust metal NCs with better performances in applications such as fluorescence sensing, biocatalysis as well as theranostic agents.

Declaration of competing interest

The authors declare that they have no known competing financial interests or personal relationships that could have appeared to influence the work reported in this paper.

Acknowledgments

This work was supported by the National Natural Science Foundation of China (No. 21705129), the Fundamental Research Fund for the Central University (Nos. 3102019jcc005, 3102019GHJD001), the Research Fund of the State Key Laboratory of Solidification Processing (NPU), China (No. 2020-QZ-01). The authors would like to thank the Analytical and Testing Center of Northwestern Polytechnical University for the TEM measurements.

Appendix A. Supplementary data

Supplementary material related to this article can be found, in the online version, at doi:https://doi.org/10.1016/j.cclet.2021.02.037.

References

[1] L. Shang, J. Xu, G.U. Nienhaus, Nano Today 28 (2019) 100767.
[2] I. Chakraborty, T. Pradeep, Chem. Rev. 117 (2017) 8208–8271.
[3] E.N. Hooley, V. Paolucci, Z. Liao, et al., Adv. Opt. Mater. 3 (2015) 1109–1115.
[4] T. Yu, C. Xu, J. Qiao, et al., Chin. Chem. Lett. 30 (2019) 660–663.
[5] C.N. Loynachan, A.P. Soleimany, J.S. Dudani, et al., Nat. Nanotechnol. 14 (2019) 883–890.
[6] W. Lan, Q. Tan, J. Qiao, et al., Chin. Chem. Lett. 30 (2019) 1627–1630.
[7] X. Bai, S. Xu, L. Wang, Anal. Chem. 90 (2018) 3270–3275.
[8] J. Xu, L. Shang, Chin. Chem. Lett. 29 (2018) 1436–1444.
[9] J. Liu, M. Yu, C. Zhou, et al., J. Am. Chem. Soc. 135 (2013) 4978–4981.
[10] M.A. Abbas, P.V. Kamat, J.H. Bang, ACS Energy Lett. 3 (2018) 840–854.
[11] Z. Wang, B. Chen, A.S. Susha, et al., Adv. Sci. 3 (2016) 1600182.
[12] Z. Wu, J. Liu, Y. Gao, et al., J. Am. Chem. Soc. 137 (2015) 12906–12913.
[13] X. Zhang, W. Liu, H. Wang, et al., Chin. Chem. Lett. 31 (2020) 859–864.
[14] Y. Zheng, L. Lai, W. Liu, et al., Adv. Colloid Interface Sci. 242 (2017) 1–16.
[15] Y. Tao, M. Li, J. Ren, et al., Chem. Soc. Rev. 44 (2015) 8636–8663.
[16] S. Chandra, Nonappa, G. Beaune, et al., Adv. Opt. Mater. 7 (2019) 1900620.
[17] J.C. Azcárate, G. Corthey, E. Pensa, et al., J. Phys. Chem. Lett. 4 (2013) 3127–3138.
[18] R. Jin, Nanoscale 2 (2010) 343–362.
[19] W. Zhong, M. Wen, J. Xu, et al., Chem. Commun. 56 (2020) 11414–11417.
[20] X. Kang, M. Zhu, Chem. Soc. Rev. 48 (2019) 2422–2457.
[21] S.E. Crawford, C.M. Andolina, A.M. Smith, et al., J. Am. Chem. Soc. 137 (2015) 14423–14429.
[22] Z. Wu, R. Jin, Nano Lett. 10 (2010) 2568–2573.
[23] S. Zhu, X. Wang, Y. Cong, et al., ACS Omega 5 (2020) 22702–22707.
[24] Y. Lin, P. Charchar, A.J. Christofferson, et al., J. Am. Chem. Soc. 140 (2018) 18217–18226.
[25] D. Shen, M. Henry, V. Trouillet, et al., APL Mater. 5 (2017) 053404.
[26] J. Liu, P.N. Duchesne, M. Yu, et al., Angew. Chem. Int. Ed. 55 (2016) 1–6.
[27] L. Wang, S. Li, J. Yin, et al., Nano Lett. 20 (2020) 5036–5042.
[28] Y. Chen, L. Li, L. Gong, et al., Adv. Funct. Mater. 29 (2019) 1806945.
[29] D. Chen, J. Li, Nanoscale Horiz. 5 (2020) 1355–1367.
[30] R.R. Nasaruddin, T. Chen, N. Yan, et al., Coord. Chem. Rev. 368 (2018) 60–79.
[31] Q. Li, M. Zhou, W.Y. So, et al., J. Am. Chem. Soc. 141 (2019) 5314–5325.
[32] J. Zheng, C. Zhou, M. Yu, et al., Nanoscale 4 (2012) 4073–4083.
[33] J.M. Forward, D. Bohmann, J.P. Fackler, et al., Inorg. Chem. 34 (1995) 6330–6336.
[34] C. Zhou, C. Sun, M. Yu, et al., J. Phys. Chem. C 114 (2010) 7727–7732.
[35] Y. Negishi, K. Nobusada, T. Tsukuda, J. Am. Chem. Soc. 127 (2005) 5261–5270.
[36] J. Jiang, C.V. Conroy, M.M. Kvetny, et al., J. Phys. Chem. C 118 (2014) 20680–20687.
[37] G. Wang, T. Huang, R.W. Murray, et al., J. Am. Chem. Soc. 127 (2005) 812–813.
[38] Q. Yu, P. Gao, K.Y. Zhang, et al., Light Sci. Appl. 6 (2017) e17107.
[39] L.Y. Chen, C.W. Wang, Z. Yuan, et al., Anal. Chem. 87 (2015) 216–229.
[40] J. Xie, Y. Zheng, J.Y. Ying, Chem. Commun. 46 (2010) 961–963.
[41] Y. Yang, L. Lu, X. Tian, et al., Sens. Actuators B: Chem. 278 (2019) 82–87.
[42] L. Shang, L. Yang, F. Stockmar, et al., Nanoscale 4 (2012) 4155–4160.